Chapter 35
Trapping Melamine with Pristine and Functionalized Graphene Quantum Dots: DFT and SERS Studies

Vaishali Sharma, Hardik L. Kagdada, Dheeraj K. Singh and Prafulla K. Jha

Abstract Present study reports structural, electronic, and surface-enhanced Raman spectroscopy (SERS) investigation of melamine on pristine and functionalized graphene quantum dots (f-GQD) using density functional theory. Structural analysis reveals that melamine is strongly adsorbed over f-GQD than pristine GQD through hydroxyl group. Adsorption energy of −0.530 eV shows the physisorption of melamine on f-GQD. HOMO–LUMO gap for pristine melamine is 5.595 eV which reduces to 1.184 eV after adsorption over f-GQD depicting the charge transfer between melamine and f-GQD. The f-GQD plays a vital role in detecting melamine through surface-enhanced Raman spectroscopy (SERS). Three peaks at 584 cm^{-1}, 680 cm^{-1}, and 736 cm^{-1} are denoted as the characteristic Raman peaks for melamine. A significant shift in Raman spectra of ~10 cm^{-1} is found after the adsorption of melamine over f-GQD. Interaction between melamine and f-GQD results in the enhancement of Raman intensities of melamine which leads to melamine detection. To evaluate SERS effect, enhancement factor (EF) is evaluated with highly intensified peak at 736 cm^{-1}. The characteristic peak of melamine at 584 cm^{-1} is increased by 396% when adsorbed over f-GQD. Our study suggests that the f-GQD is an efficient substrate for SERS effect and makes them a potential candidate for detection and sensing of melamine.

35.1 Introduction

Melamine is an organic molecule comprising 66% of nitrogen with rest of carbon and hydrogen atoms [1]. Melamine possesses benzene-like structure with three carbon and three nitrogen atoms where NH_2 group is attached to carbon atoms. This organic

V. Sharma (✉) · H. L. Kagdada · P. K. Jha
Faculty of Science, Department of Physics, The M. S. University of Baroda, Vadodara 390002, Gujarat, India
e-mail: oshivaishali@gmail.com

H. L. Kagdada · D. K. Singh
Department of Physics, Institute of Infrastructure Technology Research and Management, Ahmedabad 380026, Gujarat, India

D. K. Singh et al. (eds.), *Advances in Spectroscopy: Molecules to Materials*,
Springer Proceedings in Physics 236, https://doi.org/10.1007/978-981-15-0202-6_35

molecule is used in the manufacture process of laminates, paints, textiles, fertilizers, plastics, etc. [2, 3]. Despite these applications, it has many pitfalls, most importantly its illegal addition to the sources of protein such as milk to increase its protein content [4]. In addition, the melamine is found in some food products like animal feed and fertilizers [2, 4]. Furthermore, crystals of melamine cyanurate are found to be formed in the kidney of animals in North America, due to which several animals died because of the toxicity of this compound [5]. A combined form of melamine and its cognate cyanuric acid by hydrogen bonding were formed in the kidney and created a blockage in acute renal of dogs and cats [3, 6, 7]. All of these studies reveal that a safety mechanism such as restriction of usage and detection techniques for melamine should be developed. Some of the detection techniques have been used for detection of melamine such as gas chromatography/mass spectroscopy (GC/MS), surface-enhanced Raman spectroscopy (SERS), and colorimetric sensing methods [8–10]. GC/MS technique comes with high-priced instrumentation, while low-cost methods like electrochemical sensing are not applicable as melamine is not electroactive molecule [11]. It is a necessity to develop a detection technique that should be economical, fast, and relevant to detect melamine.

Surface-enhanced Raman spectroscopy (SERS) is one of the prominent analytical experimental techniques with extensive applications in the field of chemical production and enhancement, molecular structure and environmental invigilator [12, 13]. In SERS, the intensity of scattered Raman signal of molecule is enhanced by incorporating adsorption of molecule on metal surfaces. Two basic perceptions are characterized in SERS effect, one is chemical enhancement and other is electromagnetic enhancement [14, 15]. In electromagnetic enhancement, intensity of the Raman signal is increased by introducing electrons arrangement at the surface of molecules due to Plasmon excitation [12, 14]. While, in the chemical-enhancement phenomena, substrates or surfaces are used to increase the intensity of weak Raman signal by means of charge transfer [15]. SERS depends on several factors such as shape and size of the surface, distance between molecule and surface as well as the molecular structure (symmetry of both systems).

Graphene is the two-dimensional (2D) material with planar hexagonal structure having a large surface area and wide applications because of its economical, biocompatible, and unique electronic and dynamical properties [16]. Among carbon-based 2D materials, graphene has been extensively studied as a SERS substrate, commonly known as graphene-enhancement Raman spectroscopy (GERS). Consequently, other carbon-based nanomaterials such as graphene, graphene oxides, graphene nanoribbons, and graphene quantum dots were also utilized for SERS applications [17, 18]. However, graphene has a limitation that it can only detect 2-fold to 17-fold symmetrical molecules by SERS compared to other silicon-based substrates [19]. For that reason, zero-dimensional carbon-based material graphene quantum dot (GQD) has been utilized as it has a quantum confinement in all three directions with more adsorption of targets attributed to their excellent photoelectric properties [16, 18]. Moreover, it is a well-known fact that the functionalization of GQDs alters its structural, physical, chemical, electronic, and optical properties [20–22].

In the present study, electronic and vibrational properties of melamine on pristine and functionalized GQDs (f-GQDs) are investigated to find the better substrate for SERS of melamine. The electronic properties depict the chemical enhancement of melamine when adsorbed over pristine and functionalized graphene quantum dots (f-GQDs). The GQD is functionalized with epoxy, hydroxyl, and carboxyl groups in order to check the compatible functional group to detect the melamine.

35.2 Computational Methodology

The geometrical optimization of f-GQD and melamine is performed using first-principles-based density functional theory in order to study the structural, electronic, and vibrational properties for detection of melamine. Ground state geometries of GQD and melamine are achieved by utilizing hybrid functional Becke's three parameters together with Hartree–Fock exchange [23]. In this method, the nonlocal correlation functional is incorporated by Lee, Yang, and Parr (LYP) [24] and a local correlation developed by Vosko, Wilk, and Nusair (VWN). The 6-31G (d, p) basis set with inclusion of p- and d-orbitals is used for ground state energy calculation. All structural and vibrational properties are calculated in Gaussian09 software [25]. The structures of GQD and melamine were optimized first individually and further, for interaction between them, parallel interaction between GQD and melamine is carried out. Similar method is adopted in the case of f-GQD with melamine and this combined system is allowed to relax unless the gradient forces reach the set threshold value of 0.00045 Hartree. The adsorption energy (E_{ad}) of melamine on GQD and f-GQD is calculated by the following equation:

$$E_{ad} = E_{\text{Melamine+GQD/f-GQD}} - (E_{\text{Melamine}} + E_{\text{GQD/f-GQD}}) \tag{35.1}$$

Here, $E_{\text{Melamine+GQD/f-GQD}}$ is the total energy of the combined system of melamine and functionalized GQD, $E_{\text{GQD/f-GQD}}$ and E_{Melamine} are the total energy of individual GQD/f-GQD and melamine molecule.

35.3 Results and Discussion

35.3.1 Structural Properties

Initially, the rectangular GQD and melamine are optimized individually. Zigzag configuration of GQD and melamine structure is presented in Fig. 35.1. In GQD, the C–H and C–C bond lengths are 1.086 Å and 1.421 Å, respectively, which agrees well with the other shaped GQD [22, 26]. To examine the nature of melamine on GQD, the

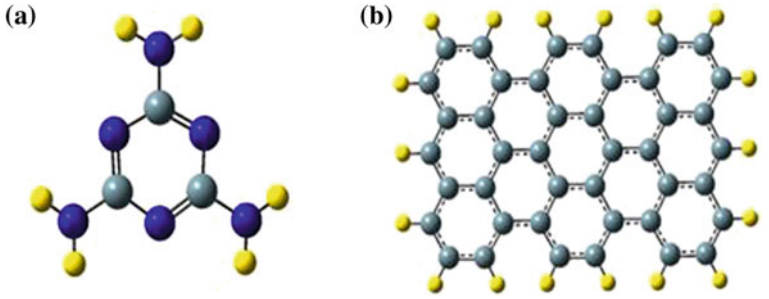

Fig. 35.1 Optimized structure of (**a**) melamine and (**b**) graphene quantum dot. Blue, grey, and yellow color balls represent nitrogen, carbon, and hydrogen atoms, respectively

adsorption mechanism is analyzed with three different sites, namely, hollow, bridge, and top.

Hollow site represents that the central hexagonal ring of melamine is initially placed at hollow position of the GQD shown in Fig. 35.2a. In the case of top site, central hexagonal ring of melamine was placed on top of the carbon atom with the distance of 1.5 Å (Fig. 35.2b), while for bridge site, central ring of melamine is placed above the middle of the bond between C–C at same distance (Fig. 35.2c).

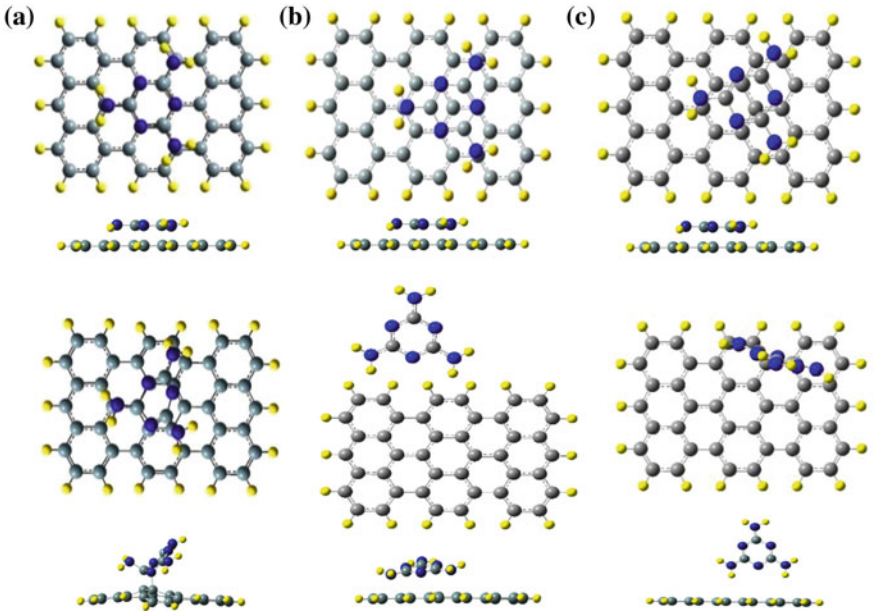

Fig. 35.2 Before and after optimization structures along with their top and side views **a** hollow melamine-GQDs, **b** top melamine-GQDs, and **c** bridge melamine-GQDs. Upper row presents before optimization and structures in lower row are after optimization

For better understanding of the geometrical change in structure of melamine and GQD, before and after optimization structures are presented in Fig. 35.2. In the case, where melamine is adsorbed at hollow site, the carbon atom of GQD is lifted up by the nitrogen atom of melamine in out-of-plane direction, while rest part of the melamine is strongly repelled by carbon atoms of GQD. This leads to positive adsorption energy of 3.98 eV. The positive adsorption energy at hollow site clearly shows the endothermic process; therefore, it is not feasible experimentally to adsorb melamine at hollow site. Melamine adsorption at top site of GQD results in the interaction of melamine at the edges of GQD through hydrogen atoms with the adsorption energy of −0.16 eV. For bridge site, the adsorption energy calculated is −0.08 eV which is almost zero. Our calculated adsorption energies are presented in Table 35.1, which reveals physisorption of melamine (top site) over pristine GQD. Further, we have investigated the adsorption of melamine by functionalization of GQD (f-GQD). Various reports suggest the modification of structural and electronic properties through functionalization [20–22].

The modification in the electronic properties will result in the chemical enhancement for better SERS effect which has been shown in one of our recent studies on another form of doped GQD, coronene [21]. Our study on the melamine over functionalized GQD will also help in understanding the better substrate for SERS (pristine or functionalized) and a compatible functional group. The different functional groups like epoxy, carboxyl, and hydroxyl were attached on GQD naming it as functionalized GQD (f-GQD). Figure 35.3 shows functionalized GQD with melamine (f-GQD-mel)

Table 35.1 Calculated adsorption energy (E_{ad}) in eV and nearest distance (d) in Å for melamine over pristine GQD and f-GQD

System	Site	E_{ad} (eV)	d (Å)
GQD + melamine	Hollow	3.98	1.50
	Top	−0.16	2.50
	Bridge	−0.08	2.90
f-GQD + melamine	Hollow	−0.53	1.88
	Top	−0.53	1.88
	Bridge	−0.53	1.88

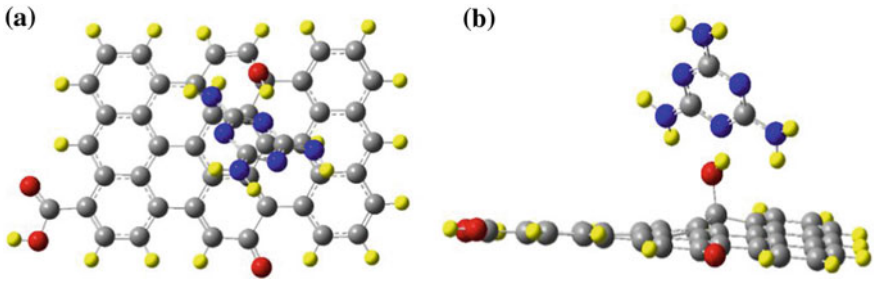

Fig. 35.3 Top and side views of optimized structure of f-GQDs-mel. The red, yellow, grey, and blue spheres represent oxygen, hydrogen, carbon, and nitrogen, respectively

after ground state optimization. The adsorption energy of −0.53 eV is same for all three sites, hollow, bridge, and top, due to their similar structural properties. This is attributed to the interaction of melamine with only hydroxyl group that leads to the homogeneous interaction for all three considered sites and results in same structural configuration. The electronic and SERS properties of melamine over f-GQD are analyzed due to the fact that adsorption energy of melamine over f-GQD is three times higher than melamine on pristine GQD.

35.3.2 Electronic Properties

To study electronic properties of melamine and f-GQD-mel, highest occupied molecular orbitals (HOMO) and lowest unoccupied molecular orbitals (LUMO) along with HOMO–LUMO gap (E_g) were investigated. Basically, HOMO has the tendency to give electrons while LUMO has potential to gain electrons. The energy separation between HOMO and LUMO distinguishes the chemical and kinetic stabilities of any molecule [27]. Frontier orbitals together with their HOMO and LUMO levels for pristine melamine and f-GQD-mel are presented in Fig. 35.4. In the case of pristine melamine, frontier orbitals HOMOs are restricted to the ring of C–N–C and

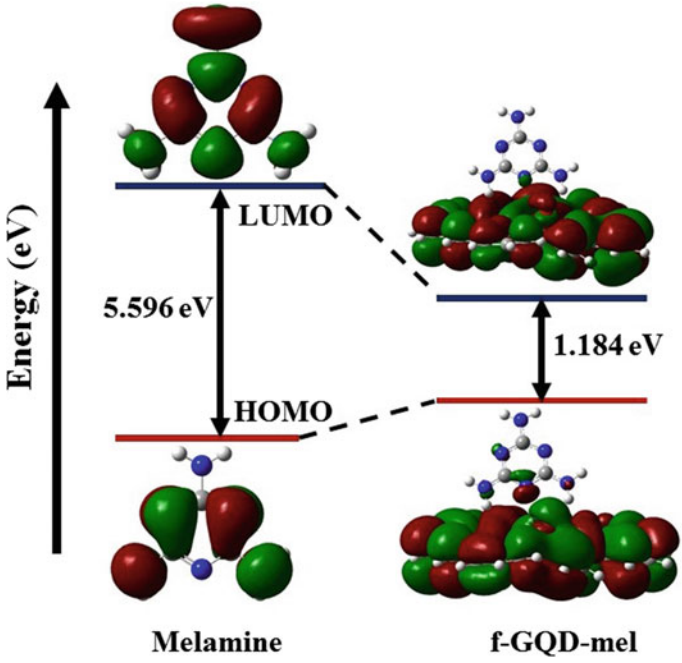

Fig. 35.4 Frontier orbitals HOMO and LUMO of melamine and f-GQD-mel

two of NH_2 groups, while LUMO levels are localized in whole melamine which can be clearly seen from Fig. 35.4. This localization of orbitals in melamine is in good agreement with previous theoretical report [28]. We have also evaluated HOMO–LUMO surfaces for f-GQD and presented in Fig. 35.4. After adsorption of melamine on f-GQD, very less amount of HOMO is localized at nitrogen atom near to functional group attributed to the physisorption of melamine on f-GQD. From Fig. 35.4, one can see that the energy gap between HOMO and LUMO levels is 5.596 eV, which further reduces after adsorption on f-GQD to 1.184 eV. The reduction in energy gap depicts strong interaction through charge transfer between the melamine and f-GQD. It should be noted that positive charge of hydrogen (interacting with nitrogen of melamine) increases from 0.28 to 0.34 e. Further, charge of nitrogen atom in melamine becomes more negative after adsorption on f-GQD. This reveals that hydrogen of epoxy group transfers negative charge to the nitrogen atom of melamine which depicts the strong interaction between melamine and f-GQD. This charge transfer will also lead to the high chemical enhancement and further results in significant SERS effect. However, this reduction in energy gap is higher than previously reported melamine with Ag nanoclusters (0.10 eV) [28]. Significant reduction in energy gap results in more charge transfer which further depicts the chemisorption in the case of reported Ag nanoclusters [28], while in our study it reveals the physisorption process.

35.3.3 SERS of Melamine

We have calculated the Raman spectra for both f-GQD-mel and pristine melamine and presented them in Fig. 35.5. We have noticed that the ring of melamine structure shows breathing at 680 cm^{-1}, which is assigned as the foremost vibrational mode for melamine. Vibrational wavenumber at 584 cm^{-1} leads to C–N–C bending along with

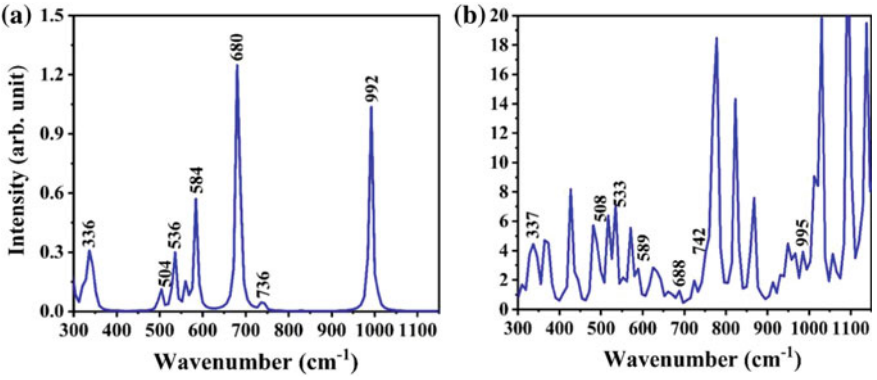

Fig. 35.5 Raman spectra of **a** pristine melamine and **b** SERS of melamine on f-GQD

the NH_2 twisting, while in the case of 736 cm^{-1}, we perceived that the melamine ring exhibits out-of-plane vibrations in which carbon atoms contribute more in the vibrational intensity than nitrogen. The three vibrational wavenumbers of melamine 584, 680, and 736 cm^{-1} have less than 10 cm^{-1} difference with available experimental results [28], which manifests consistency with experimental study. To understand SERS of melamine, we have calculated Raman spectra of melamine bounded over functionalized GQD (f-GQD). As the adsorption of melamine is negligible in the case of pristine GQD, we have studied SERS for only f-GQD with melamine. Here, it should be noted that for all three adsorption sites of melamine over f-GQD, they have similar geometry and adsorption energy of −0.53 eV (greater than melamine over pristine GQD) along with equal distance between melamine and f-GQD. These will result in identical Raman spectra with equal intensity of vibrational modes in f-GQD-mel. Therefore, we have examined and explained SERS effect for only one site. The interaction between f-GQD and melamine is determined by shift in characteristic peak of pristine melamine from 680 to 685 cm^{-1}. Another peak of 736 cm^{-1} of pristine melamine is shifted to 742 cm^{-1} when it is placed on f-GQD, which further suggests interaction of melamine over f-GQD. Wavenumbers of pristine and adsorbed melamine are tabulated in Table 35.2. The eminent significance of SERS is determined by enhancement factor (EF) of Raman activity. This factor depends on the intensity of pristine Raman spectra (I_{Raman}) and intensity of SERS spectra (I_{SERS}). We have calculated EF for all the Raman intensity observed in our calculations using following equation:

$$EF = \frac{I_{SERS}/N_{SERS}}{I_{Raman}/N_{Raman}} \tag{35.2}$$

Here, N_{SERS} is the number of molecules in SERS and N_{Raman} is the number of molecules in normal Raman. Our calculated EF for different Raman signal strengths of melamine are presented in Table 35.2. As discussed earlier, there are three basic Raman peaks obtained for melamine, in which the intensity of out-of-plane vibrational wavenumber (736 cm^{-1}) in pristine GQD is 0.046 which further enhances in f-GQD-mel up to 1.843 making highest EF of 39.890. However, the ring breathing of melamine is not affected by f-GQD which is attributed to the lack of significant

Table 35.2 Calculated Raman wavenumbers of melamine and f-GQD-mel in cm^{-1} along with enhancement factor (EF)

Melamine	f-GQD-mel	EF
336	337	14.438
504	508	16.165
536	533	23.767
584	589	4.868
680	688	1.022
736	742	39.890
992	995	2.617

change in the intensity at 680 cm^{-1} of melamine after SERS. Further, the intensity of C–N–C bending along with small amount of NH_2 twisting at 584 cm^{-1} in pristine melamine is increased in f-GQD-mel by 396%. Additionally, we have calculated EF for other Raman peaks in melamine. The intensity of twisting of NH_2 vibration in pristine melamine at 536 cm^{-1} is enhanced from 0.299 to 7.127 in SERS spectra, which gives a large EF of 23.766. While for peak obtained at 992 cm^{-1} in pristine Raman spectra of melamine (C–N–C bending), the intensity of Raman activity is enhanced by 61%. Our study of SERS reveals that among three characteristic peaks of Raman activity on melamine, two of them (584 and 736 cm^{-1}) exhibits large enhancement in SERS which will have an application in the detection of melamine.

35.4 Conclusions

In order to detect melamine, we have studied the structural, electronic, and vibrational properties of melamine adsorbed over pristine and functionalized graphene quantum dots (f-GQD) using density functional theory. Adsorption energy of melamine (−0.16 eV) suggests physisorption except at hollow site on pristine GQD, which further increases up to −0.53 eV upon the melamine adsorption on f-GQD. The adsorption distance ranges between 1.5 and 2.9 Å with the lowest at hollow site (1.5 Å shows chemisorption) in melamine over pristine GQD. While in melamine over f-GQD, the adsorption distance is same in all three sites with the value of 1.88 Å depicting similar adsorption energy. Electronic properties reveal that HOMO–LUMO gap of melamine is 5.596 eV which reduces to 1.184 eV after adsorption over f-GQD, leading to charge transfer between melamine and f-GQD. Raman spectra are analyzed in order to check the effect of surface on the Raman spectra of GQD and f-GQD and find the possibility of surface-enhanced Raman spectroscopy in melamine. Intensity of Raman wavenumbers of melamine is significantly enhanced through the adsorption over f-GQD than pristine GQD. Quantitatively, SERS effect is determined by enhancement factor (EF) of intensity of Raman wavenumbers. The highest EF of 39.89 is found for out-of-plane vibrational mode at wavenumber 736 cm^{-1}, while the intensity of the character peak of melamine at 584 cm^{-1} enhances up to 396% after adsorption over f-GQD. Calculated EF for Raman intensity of melamine is higher for all wavenumber, which depicts that the f-GQD can be a prominent material for SERS and detection of melamine.

Acknowledgements Authors acknowledge the financial assistance from the Department of Science & Technology under the Indo–Poland program of cooperation on science and technology through project DST/INT/POL/P-33/2016.

References

1. R. Muñiz-Valencia, S.G. Ceballos-Magaña, D. Rosales-Martinez, R. Gonzalo-Lumbreras, A. Santos-Montes, A. Cubedo-Fernandez-Trapiella, R.C. Izquierdo-Hornillos, Anal. Bioanal. Chem. **392**, 523–531 (2008)
2. Y. Liu, E.D. Todd, Q. Zhang, J.R. Shi, X.J. Liu, Biomed. Biotechnol. **13**(7), 525–532 (2012)
3. A.K. Hau, T.H. Kwan, P. Kam-tao, J. Am. Soc. Nephrol. **20**, 245–250 (2009)
4. C.A. Brown, K.-S. Jeong, R.H. Poppenga, B. Puschner, D.M. Miller, A.E. Ellis, K.-I. Kang, S. Sum, A.M. Cistola, S.A. Brown, J. Vet. Diagn. Invest. **19**, 525–531 (2007)
5. B. Puschner, R.H. Poppenga, L.J. Lowenstine, M.S. Filignezi, P.A. Pesavento, Diagn. Invest. **19**(6), 616–624 (2007)
6. E. Chan, S.M. Griffiths, C.W. Chan, Lancet **372**, 1444–1445 (2008)
7. Y. Cheng, Y. Dong, J. Wu, X. Yang, H. Bai, H. Zheng, D. Ren, Y. Zou, M. Li, J. Food Compos. Anal. **23**(2), 199–202 (2010)
8. H. Miao, S. Fan, Y.-N. Wu, L. Zhang, P.-P. Zhou, J.-G. Li, H.-J. Chen, Y.-F. Zhao, Biomed. Environ. Sci. **22**, 87–94 (2009)
9. T.M. Vail, P.R. Jones, O.D. Sparkman, J. Anal. Toxicol. **31**, 304–312 (2007)
10. K. Ai, Y. Liu, L. Lu, J. Am. Chem. Soc. **131**(27), 9496–9497 (2015)
11. L. Li, G. Wu, T. Hong, Z. Yin, D. Sun, E.S. Abdel-Halim, J. Zhu, A.C.S. Appl, Mater. Interfaces **6**, 2858–2864 (2014)
12. B. Zhao, R. Hao, Z. Wang, H. Zhang, Y. Hao, C. Zhang, Y. Liu, Chem. Eng. J. **349**, 581–587 (2018)
13. M. Breitman, S. Ruiz-Moreno, A.L. Gil, Spectrochim. Acta A Mol. Biomol. Spectrosc. **68**, 1114–1119 (2007)
14. X.-F. Lang, P.-G. Yin, T.-T. You, L. Jiang, L. Guo, ChemPhysChem **12**, 2468–2475 (2011)
15. B. Sharma, R.R. Frontiera, A.-I. Henry, E. Ringe, R.P.V. Duyne, Mater. Today **15**, 16–25 (2012)
16. W. Xu, N. Mao, J. Zhang, Small **9**, 1206–1224 (2013)
17. X. Yu, H. Cai, W. Zhang, X. Li, N. Pan, Y. Luo, X. Wang, J.G. Hou, ACS Nano. **5**, 952–958 (2011)
18. H. Cheng, Y. Zhao, Y. Fan, X. Xie, L. Qu, G. Shi, ACS Nano. **6**, 2237–2244 (2012)
19. X. Ling, L. Xie, Y. Fang, H. Xu, H. Zhang, J. Kong, M.S. Dresselhaus, J. Zhang, Z. Liu, Nano. Lett. **10**, 553–561 (2010)
20. P. Tian, L. Tang, K.S. Teng, S.P. Lau, Mater. Today Chem. **10**, 221–258 (2018)
21. V. Sharma, N.N. Som, S.B. Pillai, P.K. Jha, Spectrochim. Acta A **224**, 117352 (2020). https://doi.org/10.1016/j.saa.2019.117352
22. V. Sharma, N.N. Som, S.D. Dabhi, P.K. Jha, ChemistrySelect **3**, 2390–2397 (2018)
23. A.D. Becke, Phys. Rev. A **33**, 2786–2788 (1986)
24. C. Lee, W. Yang, R.G. Parr, Phys. Rev. B **37**, 785–789 (1988)
25. M.J. Frisch, G.W. Trucks, H.B. Schlegel, G.E. Scuseria, M.A. Robb, J.R. Cheeseman, G. Scalmani, V. Barone, B. Mennucci, G.A. Petersson, H. Nakatsuji, M. Caricato, X. Li, H.P. Hratchian, A.F. Izmaylov, J. Bloino, G. Zheng, J.L. Sonnenberg, M. Hada, M. Ehara, K. Toyota, R. Fukuda, J. Hasegawa, M. Ishida, T. Nakajima, Y. Honda, O. Kitao, H. Nakai, T. Vreven, J.A. Montgomery, J.E. Peralta, F. Ogliaro, M. Bearpark, J.J. Heyd, E. Brothers, K.N. Kudin, V.N. Staroverov, T. Keith, R. Kobayashi, J. Normand, K. Raghavachari, A. Rendell, J.C. Burant, S.S. Iyengar, J. Tomasi, M. Cossi, N. Rega, J.M. Millam, M. Klene, J.E. Knox, J.B. Cross, V. Bakken, C. Adamo, J. Jaramillo, R. Gomperts, R.E. Stratmann, O. Yazyev, A.J. Austin, R. Cammi, C. Pomelli, J.W. Ochterski, R.L. Martin, K. Morokuma, V.G. Zakrzewski, G.A. Voth, P. Salvador, J.J. Dannenberg, S. Dapprich, A.D. Daniels, O. Farkas, J.B. Foresman, J.V. Ortiz, J. Cioslowski, D.J. Fox, J.A. Montgomery Jr., J.E. Peralta, F. Ogliaro, M. Bearpark, J.J. Heyd, E. Brothers, K.N. Kudin, V.N. Staroverov, R. Kobayashi, J. Normand, K. Raghavachari, A. Rendell, J.C. Burant, S.S. Iyengar, J. Tomasi, M. Cossi, N. Rega, J.M. Millam, M. Klene, J.E. Knox, J.B. Cross, V. Bakken, C. Adamo, J. Jaramillo, R. Gomperts, R.E. Stratmann, O. Yazyev, A.J. Austin, R. Cammi, C. Pomelli, J.W. Ochterski, R.L. Martin, K. Morokuma, V.G.

Zakrzewski, G.A. Voth, P. Salvador, J.J. Dannenberg, S. Dapprich, A.D. Daniels, Ö. Farkas, J.B. Foresman, J. V. Ortiz, J. Cioslowski, D.J. Fox, Gaussian 09, Revision D. 01, Gaussian Inc. (2013), pp. 1–20. https://doi.org/10.1159/000348293
26. D. Raeyani, S. Shojaei, S. Ahmadi-Kandjani, **114**, 321–330 (2018)
27. K. Geetha, M. Umadevi, G.V. Sathe, P. Vanelle, T. Terme, O. Khoumeri, Spectrochim. Acta A Mol. Biomol. Spectrosc. **138**, 113–119 (2015)
28. N.T.T. An, D.Q. Dao, P.C. Nam, B.T. Huy, H.N. Tran, Spectrochim. Acta Part A Mol. Biomol. Spectrosc. **169**, 230–237 (2016)